

Functionalized gold-nanoparticles enhance Photosystem II driven photocurrent in a hybrid nano-bio-photoelectrochemical cell

Hagit Shoyhet ^{1,2,‡}; Nicholas G. Pavlopoulos ^{1,‡,‡}; Lilac Amirav ^{1,2,3,*} and Noam Adir ^{1,2,3,*,‡}

¹Schulich Faculty of Chemistry, ²The Russell Berrie Nanotechnology Institute, and ³The Nancy and Stephen Grand Technion Energy Program, Technion – Israel Institute of Technology, Haifa 32000, Israel

Supporting Information Table of contents:

1. Materials
2. SI results and figures
3. References

Supporting Information

1) Materials

HEPES (Sigma Aldrich), 2-(N-morpholino)ethansulfonic acid (MES) (Sigma Aldrich), MgCl_2 (Sigma Aldrich), NaCl (Sigma Aldrich), CaCl_2 (Sigma Aldrich), Sucrose (Sigma Aldrich), Ascorbic acid (Sigma Aldrich), EDTA (Sigma Aldrich), TritonX-100 (Sigma Aldrich), Octyl Glucoside (Anatrace), Dodecyl β maltoside (Anatrace), 2,6-Dichloroindophenol sodium salt hydrate (DCPIP) (Sigma Aldrich), Dichloro 2,6 benzoquinone (DCBQ) (Sigma Aldrich), HAuCl_3 (Sigma Aldrich), NaBH_4 (Sigma Aldrich), Cysteamine (Sigma Aldrich).

2) SI Results and Figures

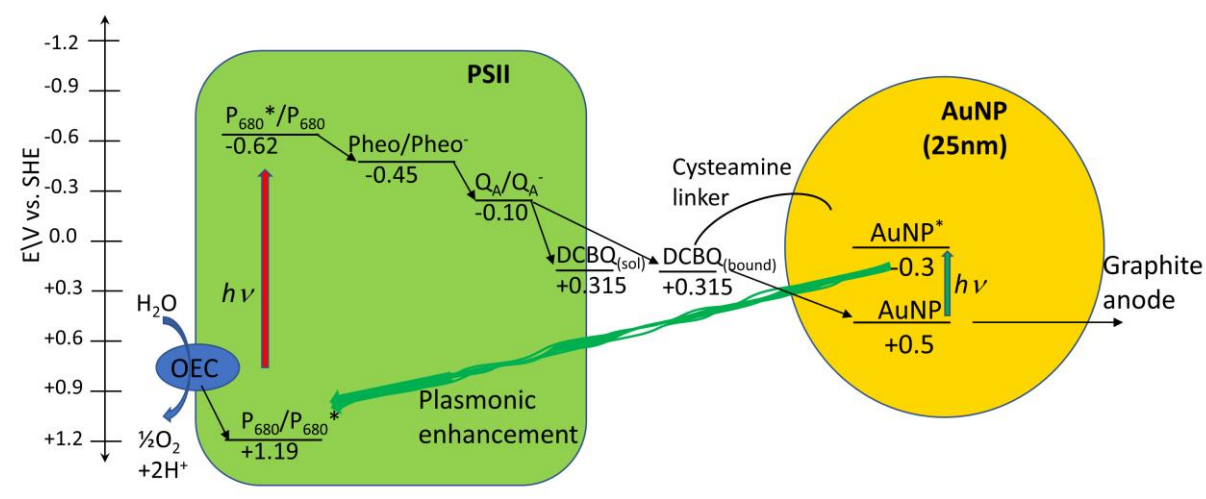


Figure S1: Schematic description of the energy levels in the PSII-AuNP_{cys}-DCBQ system. The green box and gold circle represent the PSII and AuNP_{cys}-DCBQ components, respectively. Energy levels of the AuNP are as reported in supplementary ref. 4. Thick arrows represent light-driven plasmonic enhancement activity of the AuNP at 535nm (green wavy arrow) and 660-680nm absorption of PSII (red). Electrons in PSII cascade to Q_A and then to either DCBQ bound to the AuNP through the cysteamine linker or to a small amount of soluble DCBQ. Electrons are further transferred to the BPEC graphite electrode via the AuNP which settles onto the anode.

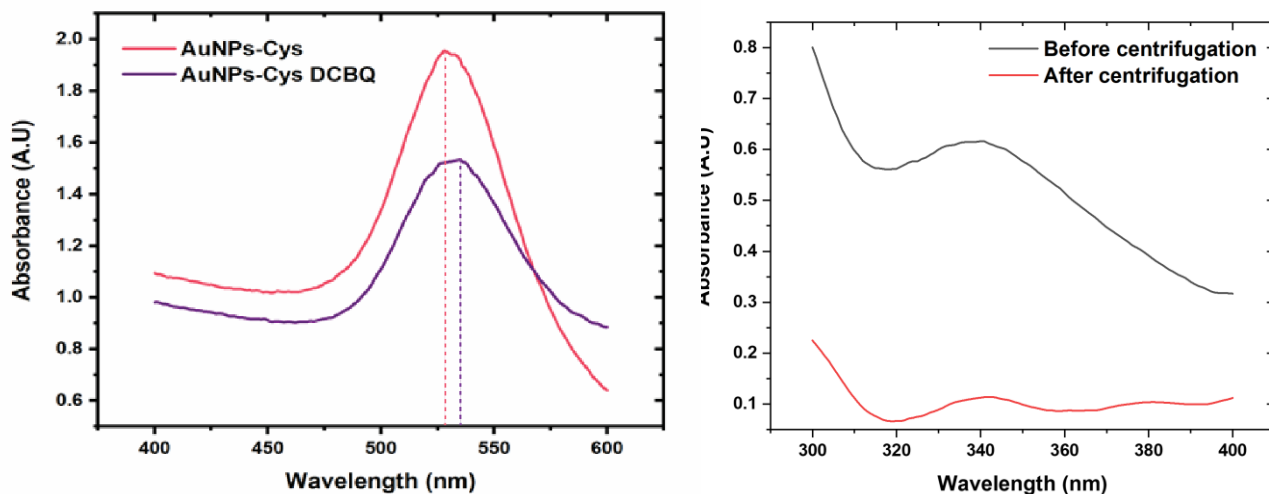


Figure S2: A. Absorbance spectra of cysteamine coated AuNPs before and after reaction with DCBQ. B. Zoom in of the absorption spectra of the supernatant of the AuNP_{cys}-DCBQ pelleted by centrifugation, showing only traces of released DCBQ. The particles were washed a second time before attaching the PSII complexes. The spectra are the average of three experiments.

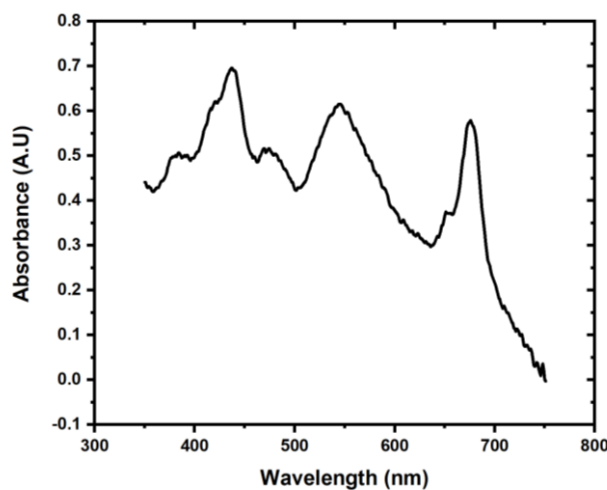


Figure S3: UV-Vis absorption of re-dispersed and washed AuNP_{cys}-DCBQ -PSII pellet. The absorption clearly showing the superposition of the chlorophyll absorption bands as well as the AuNP SPR band.

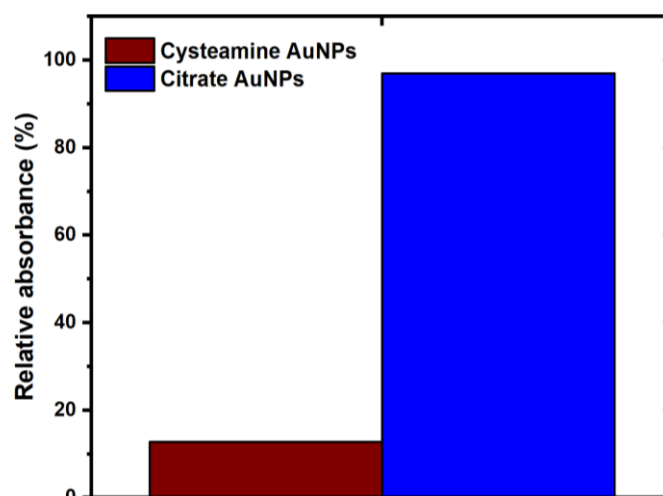


Figure S4: PSII-AuNPs conjugate connectivity is cysteamine dependent. A typical relative absorbance of the supernatant at 652 nm and maximum AuNPs concentration (1.2 nM) following centrifugation at 5000 RPM of PSII-AuNPs_{Cys-DCBQ} and PSII-AuNPs_{Citrate-DCBQ}, respectively. AuNPs with cysteamine or citrate modification were reacted with DCBQ. The resulting AuNPs_{Cys-DCBQ} or AuNPs_{Citrate-DCBQ} were mixed with PSII (see Experimental for details). 1.2 nM of the resulting PSII-AuNPs_{Cys-DCBQ} or PSII-AuNPs_{Citrate-DCBQ} were precipitated by centrifugation at 5000 rpm and the absorption of the resulting supernatants at 652nm were measured and compared to the same amount of PSII treated identically without NPS present (100%).

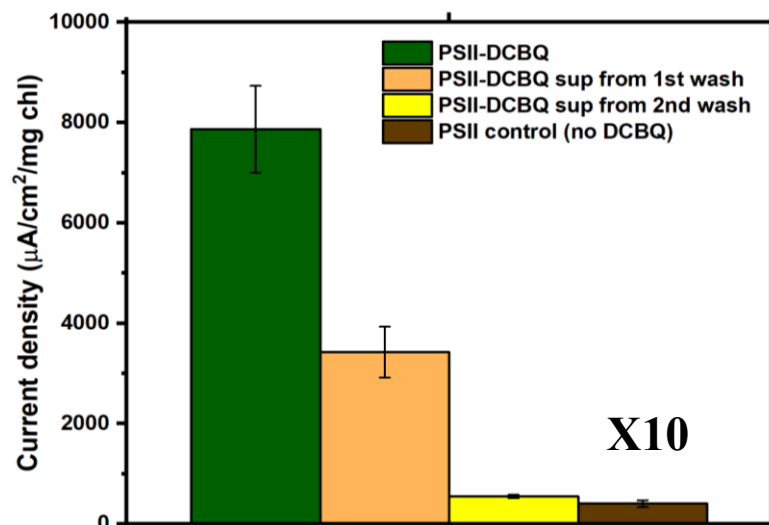


Figure S5: DCBQ binding assay. Photocurrent production from PSII after the addition of cysteamine-DCBQ capped AuNPs supernatant, post centrifugation. In order to probe for DCBQ binding efficiency to cysteamine ligand shell, DCBQ was reacted with cysteamine capped AuNPs as was described in the experimental section and washed twice by centrifugation. Each time the supernatant was saved and added to unconjugated PSII and then CA measurements were performed. The green bar represents a positive control of unconjugated PSII with the same DCBQ concentration as used to react with cysteamine capped AuNPs. The orange bar shows the photocurrent produced with the supernatant of the first wash- indicating that a fraction of DCBQ did not bind to the cysteamine on the gold nanoparticles. The yellow bar shows the remaining photocurrent produced from PSII with the supernatant from the second wash- it is clear that most of the remaining DCBQ remains firmly attached to the amine end of the cysteamine shell and does not come off. The brown bar represents PSII photocurrent without DCBQ at all or any other electron shuttle.

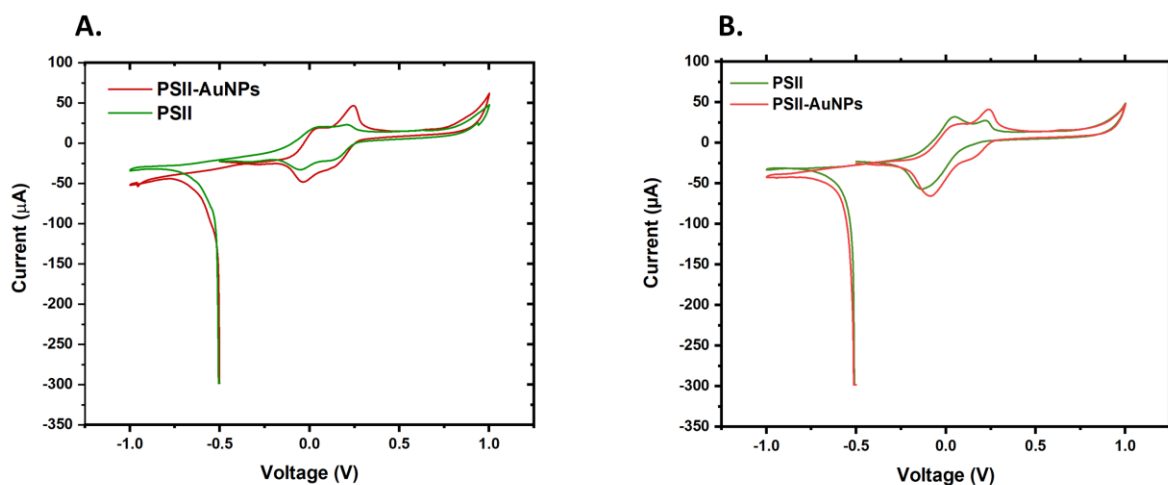


Figure S6: Cyclic voltammetry of PSII-AuNPs with conjugated PSII or unconjugated PSII, in solution. A) CV measured during constant illumination. B) CV measured in the dark. Samples were scanned at a rate of 0.1 V/s ranging from -1V to 1V. Illumination was performed with white light at an intensity of 250mW/cm².

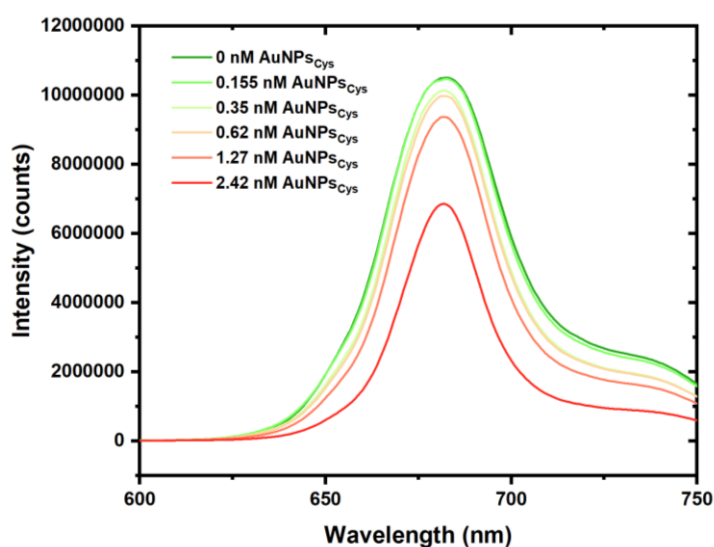


Figure S7: PSII fluorescence quenching in the absence of DCBQ modification of AuNP_{Cys}. Fluorescence of PSII was measured in the presence of AuNP_{Cys} lacking the DCBQ modification, shows reduced quenching when compared to the results presented in Fig. 2.

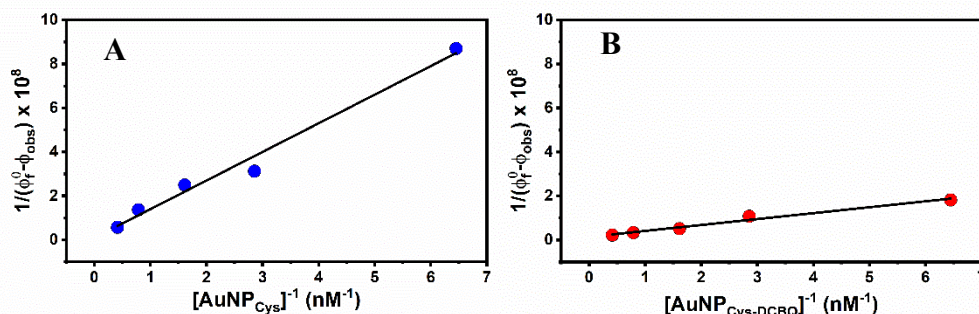


Figure S8: Examination of the role of DCBQ in electronic connectivity in PSII-AuNPs conjugate. Double reciprocal analysis comparison for fluorescence quenching of PSII excited state by A) $AuNP_{Cys}$ and B) $AuNP_{Cys-DCBQ}$.

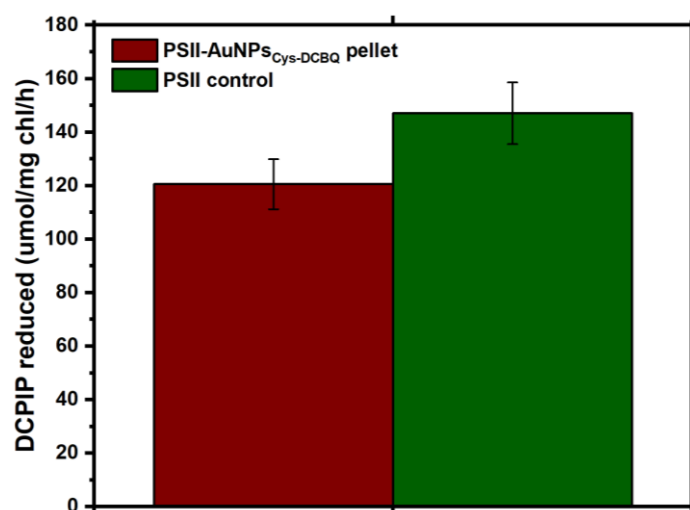


Figure S9: PSII removed from PSII-AuNPs are still active. PSII-AuNPs conjugates containing the highest AuNPs DCBQ concentration (7.6 μM) were precipitated as described in the centrifugation binding assay. The pellet was then resuspended in MES buffer containing 0.05% Dodecyl β maltoside in order to remove the PSII complexes from the NPs. DCPIP to final concentration of 7 μM was added to the solution, and the absorbance at 600nm was measured in the dark. The reaction mixture was then illuminated with white light for 20 seconds and incubated in the dark for additional 40 seconds, after which absorbance at 600 nm was measured again. The activity was calculated according to Beer-Lambert law and the extinction coefficient of DCPIP.¹

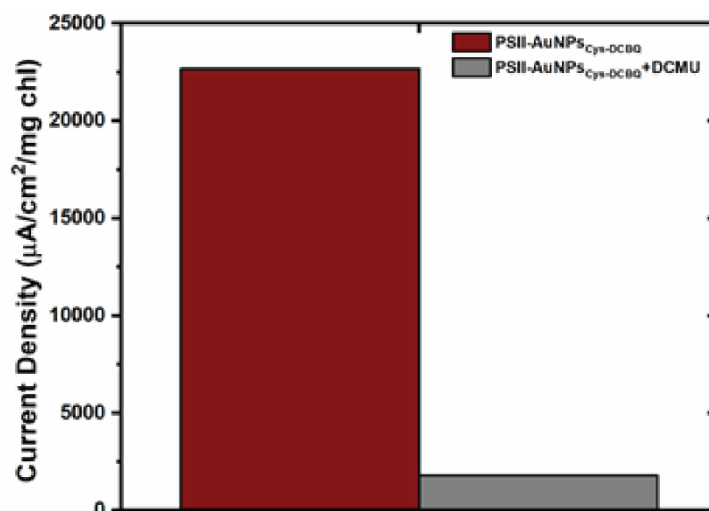


Figure S10: PSII-AuNPs conjugate photocurrent is inhibited by DCMU. The herbicide DCMU inhibits electron transfer to the Q_B site in PSII. We performed CA measurements as in Fig. 3, in the presence of DCMU to assure that the current is still PSII dependent. The red bar presents photocurrent produced by PSII-AuNPs conjugate and the grey bar presents the photocurrent produced by the conjugate in the presence of 10 µM DCMU.^{2,3}

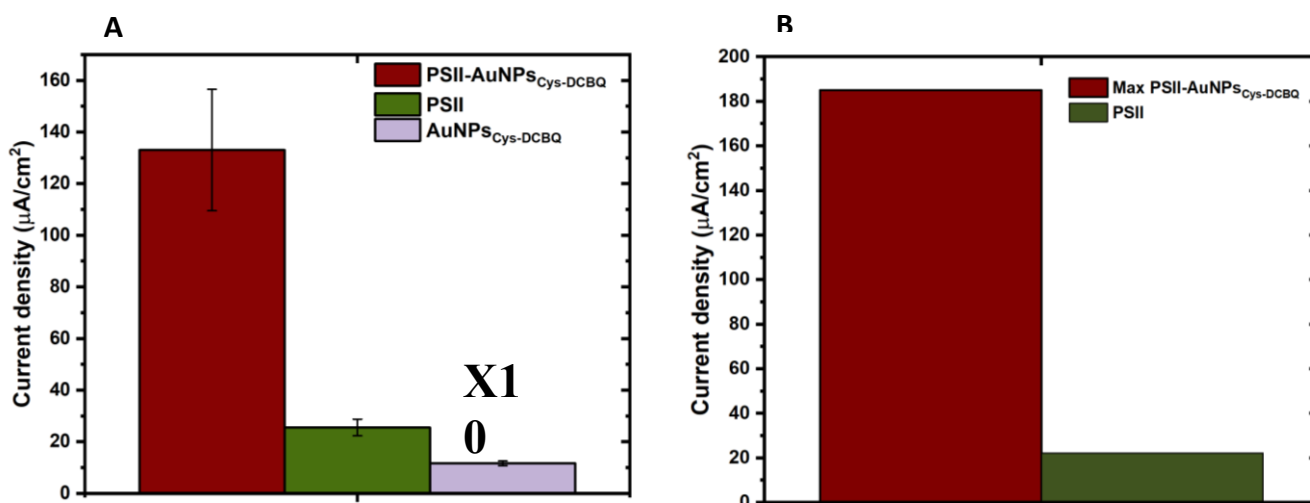


Figure S11: Absolute PSII-AuNPs conjugate photocurrent values A: Average PSII-AuNP_{Cys-DCBQ} conjugate photocurrent density values, without normalization to mg chlorophyll. B: Maximal photocurrent achieved with PSII-AuNPs conjugate compared to bare PSII photocurrent showing near to 10X increase in photocurrent. In order to compare the photocurrent value produced by cysteamine-DCBQ AuNPs to that of PSII control and PSII-AuNPs, we show in Figure S10 the absolute current density values for the conjugate, as well as the controls

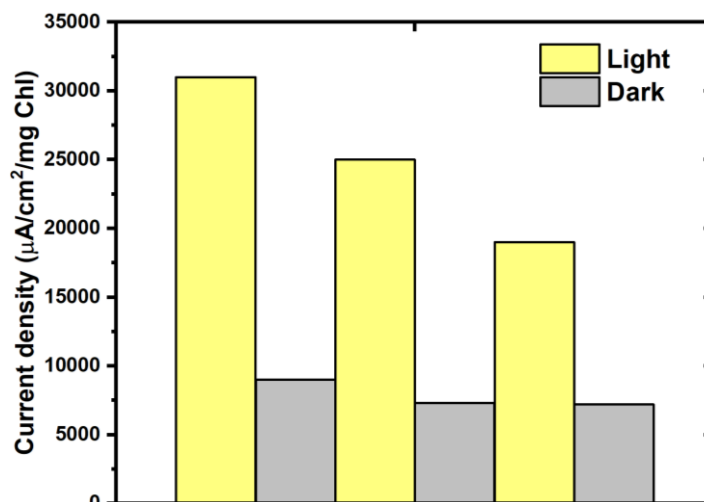


Figure S12: Light-Dark photocurrent measurement. A typical PSII-AuNPs conjugate photocurrent measurement in light-dark cycles. The yellow bars represent maximum normalized currents under illumination, the grey bars represent normalized dark currents after stabilization and reaching a plateau.

SI Table 1: Tri-exponential fitting parameters and amplitude weighted average lifetimes of the TCSPC measurements for PSII and PSII-NP conjugates.

Sample	A ₁ (%)	τ_1 (ps)	A ₂ (%)	τ_2 (ps)	A ₃ (%)	τ_3 (ps)	τ_{avg} (ns)
PSII	5.71	563.3	53.05	3156.1	41.24	5665.7	2.6
PSII+AuNP _{Cys}	5.39	451.6	45.31	2975.1	49.30	5433.6	2.3
PSII+AuNP _{Cys} -DCBQ	3.69	136.3	21.1	1553.3	75.3	4807.3	1.2

References

1. O. Kolaj-Robin, S. R. O'Kane, W. Nitschke, C. Léger, F. Baymann and T. Soulimane, *Biochimica et Biophysica Acta (BBA) - Bioenergetics*, 2011, **1807**, 68-79.
2. D. Kirilovsky, A. W. Rutherford and A. L. Etienne, *Biochemistry*, 1994, **33**, 3087-3095.
3. A. Trebst, in *Methods Enzymol.*, Academic Press, 1972, vol. 24, pp. 146-165.
4. S. Barazzouk, P. V. Kamat and S. Hotchandani, *J. Phys. Chem. B*, 2005, **109**, 716-723.